7th Australasian Hydraulics and
Fluid Mechanics Conference,
Brisbane, 18-22 August, 1980

Flow Phenomena of Polymer Solutions in an Annular Die

C. TIU
Senior Lecturer, Department of Chemical Engineering, Monash University
and
K.L. TAN
Senior Process Engineer, Esso Australia Limited, Victoria

SUMMARY The dynamic behaviour of the entry flow of viscoelastic polymer solutions in an annular die was studied using a cine film. Several flow patterns on the upstream side of the contraction were observed depending upon the relative magnitudes of elastic and inertial forces. The flow could be classified into stable and unstable flows. The stable flow was characterised by an initial growth of vortex size near the corner of the contraction followed by a reduction in cell size until first-stage instability was reached. The unstable flow regime exhibited initially a first-stage disturbance, characterised by low frequency disruption of vortices, then a metastable region, and finally a high frequency random distortion of flow field. The onset of flow instability occurred at an Elasticity number of around 0.03 to 0.035.

1 INTRODUCTION

The polymer processing industry is one of the most important industries where viscoelastic fluids are encountered. There have been many publications dealing with flow behaviour of polymer melts and solutions in the die entry and the mechanisms governing the onset of flow instability. Most studies are concerned with the entry flow in circular ducts. One geometry which has received very little attention is the annulus despite its increasing importance in extrusion, wire coating, film blowing and moulding.

The aim of this study is to experimentally investigate the upstream entry flow behaviour of viscoelastic polymer solutions in an annular die entry. Flow patterns are recorded in motion pictures. Various flow regimes are identified and correlated with fundamental fluid parameters, and the condition for the onset of flow instability is established.

2 EXPERIMENTAL AND DATA ANALYSIS

Flow visualisation experiments were carried out in a closed loop flow system. Details of the experimental set-up and procedure have been described elsewhere (Tan, 1977, Tan and Tiu, 1977). Visualisation of flow field was achieved through the use of an optical technique involving streak photography. The transient behaviour of entry flow patterns was recorded on a 16-mm cine film. A 16-mm Pentaflex AK16 cine camera, fitted with a 15-200 mm zoom lens was used. The film used was Ilford Mark V (type 782), with a nominal film speed of 400 ASA. A special developer, Acufine (Acufine Inc., Chicago) was used to increase the film speed 4-fold to 1600 ASA. Such a high film speed was necessary to obtain good photographic images due to the low reflected light intensity from the tracer particles. Most of the filming was done at a speed of 16 frames/sec.

The test fluids were dilute aqueous solutions of Methocel 90HG (hydroxypropyl methyl cellulose), Separan AP30 and MG500 (partially hydrolysed polyacrylamide) from Dow Chemicals. Varying concentrations were used to give a wide range of viscous and elastic properties. The code names FM and FS used herein denote Methocel and Separan solutions respectively.

The viscometric data were fitted with power-law models,

$$\tau = K\dot{\gamma}^n \tag{1}$$

and

$$N_1 = P_{11}-P_{22} = \sigma\dot{\gamma}^s \tag{2}$$

For greater accuracy some of the flow curves were approximated with two power-law regions over the experimental shear rate range. The fluid parameters n, K, σ and s for test fluids used in the cine film work are tabulated in Table 1. In the data analysis and correlation, three dimensionless groups, representing various force ratios, were introduced (Tan and Tiu, 1977, 1979):

Reynolds number,

$$Re = \frac{2^{3-n} r_H^n \langle u\rangle^{2-n} \rho}{K[(\varepsilon_o n+\varepsilon_1)/n]^n} = \frac{\text{inertial force}}{\text{viscous force}} \tag{3}$$

Weissenberg number,

$$Ws = \frac{\sigma}{K}\left[\frac{\langle u\rangle}{r_H}\right]^{s-n} = \frac{\text{elastic force}}{\text{viscous force}} \tag{4}$$

Elasticity number,

$$\xi = Ws/Re = \frac{\text{elastic force}}{\text{inertial force}} \tag{5}$$

The experimental conditions and the sequence of the cine film are given in terms of these dimensionless groups, as shown in Table 2.

3 DISCUSSION OF RESULTS

The annular entry flow geometry is represented schematically in Figure 1. The origin of the x-coordinate is at the contraction plane. L_v represents the vortex detachment length, which is defined as the negative of the x-coordinate where the flow detaches from the outer annular wall. The stationary vortex length is expressed in dimensionless form as

$$X_v = -L_v/4R_H \tag{6}$$

where R_H is the hydraulic radius of the annulus upstream of the contraction.

Following the sequence of the cine film, the flow of viscoelastic polymer solutions into an annular

die can be broadly classified into a *stable* and an *unstable* flow regime.

3.1 Stable Flow

The stable flow regime can be further divided into a vortex growth region and a divergent flow region depending upon the magnitudes of Reynolds and Elasticity numbers. At low Reynolds numbers (refer to Sequence 1*, Re = 8.0), the flow field is characterised by the presence of a stationary vortex at the upstream corner of the contraction. As the flow rate increases (Re = 14.7 in Sequence 2), the vortex size also increases, accompanying by a faster recirculation rate within the vortex cell. The bulk of the fluid accelerates smoothly into the downstream annulus in a funnel-shaped pattern. The term *vortex growth* is used to describe this flow region. Although an increase in Reynolds number results in a decrease in Elasticity number, in the vortex growth region the elasticity level is still sufficiently high to have a major influence on the flow field. This is manifested in the form of a stored elastic energy, which increases with increasing Reynolds number. This energy is thought to be responsible for the occurrence of the stationary vortex.

In order to establish that fluid elasticity is the dominant factor behind the presence of a large stationary vortex, the flow pattern is compared with that observed for an inelastic fluid having similar viscous characteristics and Re values. The inelastic fluid used is FM1 with n = 0.862 and K = 0.196 N-sec^n/m^2. It is evident from Sequence 3 that the flow of an inelastic fluid into an annular contraction is purely radial. There is no discernable secondary vortex at the corner of the contraction plane even at such low Reynolds number (Re = 4.5) where the influence of axial diffusion of momentum is expected to be significant. In a recent theoretical study, Perera and Walters (1976) found the effect of shear thinning to be of secondary importance. It can be concluded that the occurrence of a large stationary vortex in an abrupt annular entry is a manifestation of fluid elasticity. This, however, does not preclude the effect of fluid inertia since all experimental conditions exceed the creeping flow limit. In the vortex growth region, it simply indicates that the rate of growth of secondary cell as a result of fluid elasticity is far greater than the rate of diminishing in cell size due to fluid inertia.

When the Reynolds number reaches certain critical values, about Re = 10, the vortex attains its maximum size. Further increase in Reynolds number results in an abrupt change in the nature of the flow pattern. Sequence 4 shows that at Re = 162 and ξ = 0.0493, the streaklines near the outer wall diverge out towards the solid boundary as the vortex detachment plane is approached. The forcing of bulk fluid into the secondary cell results in a reduction in cell size. This region of flow is termed *divergent flow*. The predominant force influencing the flow field in this region is the fluid inertia, as indicated by the low value of ξ.

The variation of the vortex size with Reynolds number is shown for Fluid FS8 in Figure 2. Each data point represents at least ten measurements of L_y on both halves of the annulus from streakline photographs. The vortex growth and divergent flow regions are well defined, with the maximum vortex size occurring at a critical Re of around 10. Similar phenomena have been found for circular die (Cable and Boger, 1978).

3.2 Unstable Flow

The characteristics of unstable flow in an annulus are studied using three viscoelastic fluids, FS5, FS7 and FS8. Flow patterns obtained for the inelastic fluid, FM1, are compared with those of the viscoelastic fluids to illustrate the effect of fluid elasticity. Since results are obtained from fluids of different viscosities and levels of elasticity, much emphasis is placed on the Elasticity number ξ in the correlation of flow regimes.

A common feature of all viscoelastic fluids flowing in the annular contraction is that increasing the flow rate beyond the divergent flow region, a transition point is reached where a first stage disturbance to the stable flow occurs. This transition point, occurring at ξ at about 0.03 to 0.035, may be taken as the critical point which marks the onset of unstable flow. In this narrow range of ξ there is a low frequency random disruption of stationary vortex. The vortex is observed to break and then reform in a random fashion (Sequence 5). Unlike the grossly unstable flow behaviour observed for LDPE melts (Bagley and Birks, 1960; Ballenger and White, 1971), where the central filament entering a circular die breaks and retracts while the material from the corner vortex surges into the die, the polymer solutions display only a partial disruption of the main flow in the annulus.

At slightly lower Elasticity numbers, and higher Reynolds numbers, a metastable flow region observed. This region occurs between $0.025 \leq \xi \leq 0.03$. Four different multiple flow patterns are observed at similar flow conditions (Sequences 6 to 9). Each flow pattern has been found to persist for as long as half an hour. Two of the flow patterns are symmetric while the other two are asymmetric.

The symmetric flow observed with fluid FS7 exhibits two flow patterns occurring at almost identical experimental conditions, ξ = 0.028 and 0.0285 and Re = 157 and 152. One flow pattern shows no significant stationary vortex. Fluid elements arriving in the vicinity of the 90^{o}corner bend rapidly and accelerate radially along the wall of the contraction plane into the smaller annulus. No disruption of streamlines at the entry is evident. The other flow pattern shows a distinct region of secondary cell at the 90^o corner. The bulk of the fluid converges smoothly into the smaller annulus, with the fluid elements near the boundary between the bulk flow and the stationary vortex accelerate rapidly into the entry.

The asymmetric flow patterns, which may be regarded as mirror images of one another, seem to arise from a combination of the two symmetric flow patterns. One half of the flow field exhibits purely radial flow, while the other shows a distinct secondary vortex at the corner of the contraction. These peculiar flow patterns occur only at slightly higher Reynolds numbers, $160 \leq Re \leq 200$, or lower ξ values, $0.028 \leq \xi \leq 0.026$.

Proceeding to higher Reynolds numbers and lower Elasticity numbers, $\xi < 0.025$, a second stage flow instability is observed. This second stage instability is characterised by high frequency random distortions of the flow field just upstream of the contraction. (Sequences 10 and 11). The flow is chaotic and the frequency of distortions

* The film "Flow Patterns in Abrupt Annular Entry Flow of Viscoelastic Fluids" is available for loan, Department of Chemical Engineering, Monash University.

increases with increasing Reynolds number. In view of the high Reynolds number and low Elasticity number encountered in this flow regime, the flow instability is clearly an inertia-induced process. This flow instability is completely different from the grossly disrupted flow patterns reported for polymer melts at low Reynolds numbers, where inertial effects are negligible (Ballenger and White, 1971).

4 ACKNOWLEDGMENTS

The authors wish to acknowledge the financial support received from the Australian Research Grants Committee. One of us (K.L. Tan) also wishes to thank Monash University for the award of Graduate Scholarships during the course of his postgraduate study.

5 NOTATION

K,n,s,σ	power law parameters
L_v	vortex detachment length
$N_1=P_{11}-P_{22}$	first normal stress difference
P_{ii}	deviatoric normal stress, i = 1,2
r_1	inner radius of downstream annulus
r_2	outer radius of downstream annulus
R_2	outer radius of upstream annulus
r_H	$(r_2-r_1)/2$, hydraulic radius of downstream annulus
R_H	$(R_2-r_1)/2$, hydraulic radius of upstream annulus
$\langle u \rangle$	average velocity in downstream annulus
X_v	dimensionless detachment length defined in eqn. (6)
Re	Reynolds number defined in eqn. (3)
Ws	Weissenberg number defined in eqn. (4)
$\varepsilon_o, \varepsilon_1$	geometric parameters
$\dot{\gamma}$	steady shear rate
τ	steady shear stress
ρ	density

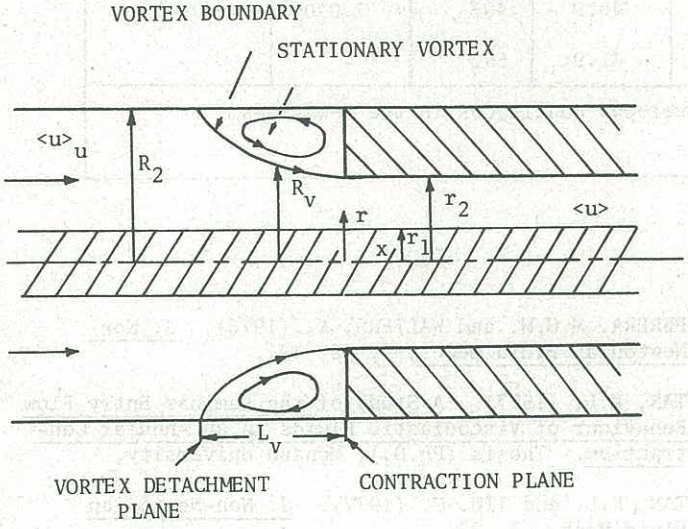

Figure 1 Schematic Diagram of Annular Entry Geometry

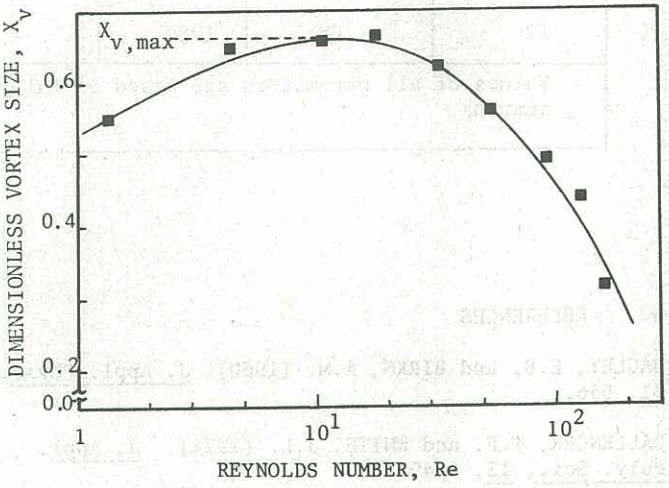

Figure 2 Dimensionless vortex size as a Function of Reynolds Number

TABLE I

POWER-LAW MODEL PARAMETERS FOR SHEAR STRESS AND FIRST NORMAL STRESS DIFFERENCE DATA FOR TEST FLUIDS USED IN THE CINE FILM WORK

Fluid	n	K(N sec^n/m^2)	$\dot{\gamma}$ (sec^{-1})	s	σ(N sec^n/m^2)	$\dot{\gamma}$ (sec^{-1})	Temp.(^oC)
FS5	0.436	2.066	176-1112	0.914	0.947	443-1112	22
FS7	0.412	1.514	4.4-176	0.683	2.789	4.4-442	15.7
	0.48	1.070	176-1112	0.984	0.433	442-1112	15.7
FS8	0.367	4.46	4.4-222	0.633	9.269	17.6-222	16.0
	0.397	3.914	222-1112	0.758	4.667	222-1112	16.0
FM1	0.862	0.196	4.4-71	-	-	-	13.5
	0.628	0.521	71-894	-	-	-	13.5

TABLE II

EXPERIMENTAL CONDITIONS FOR CINE FILM WORK

Sequence Number	Fluid	$\dot{\gamma}(sec^{-1})$	$N_1(N/m^2)$	$\tau(N/m^2)$	Re	Ws	ξ
1	FS7	73.3	52.4	8.9	8.0	3.964	.496
2	FS8	198.6	264.3	31.1	14.7	5.651	.384
3	FM1	22.4	-	2.86	4.5	-	-
4	FS8	856	779.7	57.1	162	7.979	.0492
5	FS8	1286	1062	67.1	312	9.242	.0296
6	FS7	454	177.5	20.2	157	4.390	.0280
7	FS7	443	173.4	19.9	152	4.337	.0285
8	FS7	461	180.8	20.3	161	4.425	.0275
9	FS5	728	391.6	36.6	202	5.380	.0266
10	FS7	735	284.7	25.4	312	6.263	.0201
11	FS5	1286	658.8	46.9	493	7.070	.0143
12	FM1	1080	-	41.9	552	-	-

Values of all parameters are based on fully developed conditions in the downstream annulus.

6 REFERENCES

BAGLEY, E.B. and BIRKS, A.M. (1960). J. Appl. Phys., 31, 556.

BALLENGER, T.F. and WHITE, J.L. (1971). J. Appl. . Poly. Sci., 15, 1949.

CABLE, P.J. and BOGER, D.V. (1978) A.I.Ch.E.J. 24 869, 992.

PERERA. M.G.M. and WALTERS, K. (1976). J. Non-Newtonian Fluid Mech., 2, 49, 191.

TAN, K.L. (1977). A Study of the Laminar Entry Flow Behaviour of Viscoelastic Fluids in an Annular Contraction. Thesis (Ph.D.), Monash University.

TAN, K.L. and TIU, C. (1977). J. Non-Newtonian Fluid Mech., 3, 25.

TAN, K.L. and TIU, C. (1979) ibid, 6, 21.